Received: 5 March 2021 | Revised: 4 April 2021 | Accepted: 6 April 2021

DOI: 10.1002/ardp.202100092

FULL PAPER

ARCH PHARM DPhG
Archiv der Pharmazie

Synthesis of 5*H*-indeno[1,2-*b*]pyridine derivatives: Antiproliferative and antimetastatic activities against two human prostate cancer cell lines

Katiuska E. Charris[1] | Juan R. Rodrigues[2] | Hegira Ramírez[1,3] | Esteban Fernandez-Moreira[4] | Jorge E. Ángel[5] | Jaime E. Charris[1]

[1]Organic Synthesis Laboratory, Faculty of Pharmacy, Central University of Venezuela, Caracas, Venezuela

[2]Departamento de Tecnología de Procesos Biológicos y Bioquímicos, División de Ciencias Biológicas, Universidad Simón Bolívar, Caracas, Venezuela

[3]Facultad de Medicina, Universidad de Las Américas, Quito, Ecuador

[4]Escuela de Medicina, Universidad Espíritu Santo, Samborondón, Ecuador

[5]Organic Synthesis Laboratory, Design and Pharmacological Evaluation of New Products, Experimental Faculty of Science, Central University of Venezuela, Zulia University, Maracaibo, Venezuela

Correspondence
Jaime E. Charris, Organic Synthesis Laboratory, Faculty of Pharmacy, Central University of Venezuela, 47206, Los Chaguaramos 1041-A, Caracas, Venezuela.
Email: jaime.charris@ucv.ve

Abstract

This study describes the direct synthesis of 2-amino-4-(phenylsubstituted)-5*H*-indeno[1,2-*b*]pyridine-3-carbonitrile derivatives **5**–**21**, through sequential multicomponent reaction of aromatic aldehydes, malononitrile, and 1-indanone in the presence of ammonium acetate and acetic acid (catalytic). The biological study showed that compound **10** significantly impeded proliferation of the cell lines PC-3, LNCaP, and MatLyLu. The antimetastatic effects of compound **10** could be related with inhibition of MMP9 in the PC-3 and LNCaP human cell lines. On the basis of a study of the structure–activity relationship of these compounds, we propose that the presence of two methoxy groups at positions 6 and 7 of the indeno nucleus and a 4-hydroxy-3-methoxy phenyl substitution pattern at position 4 of the pyridine ring is decisive for these types of molecules to exert very good antiproliferative and antimetastatic activities.

KEYWORDS
anticancer, antimetastatic, antiproliferative, indeno, prostate, pyridine

1 | INTRODUCTION

Cancer is the second leading cause of death globally after ischemic heart disease and stroke. In 2018, there were an estimated 18.1 million new cases and 9.6 million deaths from cancer, as per data registered by the World Health Organization (WHO).[1] The most frequently diagnosed cancer was of the lung, followed by female breast cancer and colorectal cancer.

The American Cancer Society estimated that the number of new cancer cases and deaths in the United States of America, by 2021, will be in the order of 1,898,160 and 608,570, respectively.[2] On the basis of expected population growth and aging along, the incidence and mortality rates from cancer are expected to increase by 60% by 2040.[3]

Prostate cancer (PCa) is the second most common cancer among men in the United States and the fifth most common cancer worldwide; however, incidence and mortality of this disease differ greatly depending on the geographical area.[2] Although there are several types of cancer treatment options in practice, their success depends on the type and stage of cancer. However, they have limitations. To date, chemotherapy has played a central role in the clinical treatment of cancer, and numerous anticancer agents have been approved for this purpose.[4-6]

In the clinical treatment of PCa, the strategy of inhibition of the function of androgen receptors, established in the 1940s, is used.[7] Although the disease is at first sensitive to androgen deprivation therapy, the majority of patients eventually progress to a stage termed castration-resistant prostate cancer.[8] Therefore, a new

rational approach to finding new drugs and new targets of action for PCa treatment is needed. Among those nucleos that have shown promising results, we can point to the bicalutamide, isoxazolones, pyrrole carboxamides, pyridines and *N*-arylpiperazine derivatives, indeno[1,2-*d*]pyrimidine-5-one, imide-based analogs, hydantoin, benzochromene, benzoquinoline, quinoline, coumarin derivatives, and organometallic-containing derivatives.[9-14]

One of those investigated targets with a renewed interest in recent years is matrix metalloproteinases (MMPs), listed as a large family of zinc-dependent endoproteases known to exert multiple regulatory roles in proliferation, adhesion, migration, and invasion of cancer cells as well as in angiogenesis in the tumor.[15-18] Two of these MMPs, MMP2 and MMP9, known as gelatinases A and B, respectively, are found in many human malignancies, including skin, prostate, pancreas, breast, brain, colon, and lung, and are often correlated with tumor aggressiveness and poor prognosis.[19-21]

According to recent reports, it has been found that quinolinyl acrylates,[22] 2-amino-5,6-dihydro-4-phenylbenzo[*h*]quinoline-3-carbonitrile,[11] 2-amino-4-benzylpyridine-3-carbonitrile,[9] 2-amino-4-quinolinyl-naphthopyran-3-carbonitrile,[12] natural alkaloids like onychnine and polyfothine or 2-amino-4-phenyl-5*H*-indeno[1,2-*d*]pyrimidine-5-one derivatives,[10,23] and 6,7-dimethyl-4-(3,4,5-trimethoxyphenyl)-3,4-dihydroquinolin-2(1*H*)-one (DTDQ)[24] are particularly active as anticancer and MMP inhibitors. This literature reveals that 1,2-dihydronaphthalene and 1*H*-indene-coupled heterocyclic compounds possess remarkable anticancer activity. On this basis, and as a continuation of previous work,[11,22] we are reporting for the first time the synthesis and characterization of 2-amino-4-phenylsubstituted-5*H*-indeno[1,2-*b*]pyridine-3-carbonitrile derivatives, via a one-pot synthesis from elementary starting materials as 1-indanone methoxy-substituted, aromatic aldehydes-substituted, malononitrile, ammonium acetate, and acetic acid (catalytic) in toluene, and their evaluation as potential anticancer agents against human PCa cells PC-3 and LNCaP in vitro. Inhibitory effects were also observed on the adhesion, migration, and invasion of the PCa cells as well as on clonogenic activity, possibly by inhibition of MMP-9 activity.

2 | RESULTS AND DISCUSSION

2.1 | Chemistry

Due to the importance of these kinds of compounds, the synthesis of 2-aminopyridine derivatives has been largely investigated[25-28]; however, the development of a general and efficient synthetic strategy to obtain 2-aminopyridine fused with a five-membered ring of the indene is still desired. In a pilot reaction, benzaldehyde-substituted **1** (1 mmol), malononitrile **2** (1 mmol), 1-indanone-substituted **3** (1 mmol), and ammonium acetate (1.5 mmol) in toluene (10 ml), with catalytic amount of acetic acid, were combined in a 20-ml round-bottom flask fitted with a reflux condenser equipped with a Dean–Stark trap (Scheme 1a). The resultant reaction may be assumed to proceed via the Knoevenagel reaction with the formation of arylidenemalononitrile **4**, which then undergoes Michael addition with 1-indanone respective **3**, followed by cyclization, isomerization, and aromatization to obtain the final products **5**–**21** (Scheme 2). The reaction mixture was then poured into crushed ice. The solid product was filtered by suction and washed with a mixture of water–ethanol. The analytical and spectral data of compounds **5**–**21** were consistent with their respective structures.

The infrared (IR) spectra of the compounds show two characteristic bands between 3392 and 3312, and 3328 and 2976 cm^{-1}, confirming the presence of –OH and $–NH_2$.

Furthermore, between 2224 and 2192 cm^{-1}, stretching vibration indicates the presence of –CN group, and between 1603 and 1596 cm^{-1}, stretching vibration indicates the presence of –N═C– of the heterocyclic group. In the ^1H nuclear magnetic resonance (NMR) spectrum, a singlet (s) is observed that appears between 3.35 and 3.86 ppm, assigned to the two protons at position 5 of this family of compound 5*H*-indeno[1,2-*b*]pyridine. The remaining aromatic

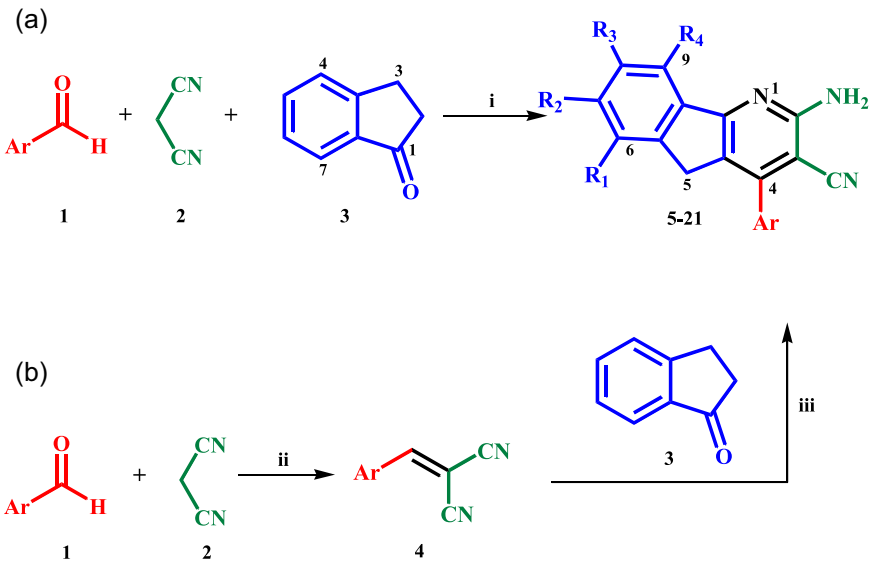

SCHEME 1 (a) Three-component process for the synthesis of 5*H*-indeno[1,2-*b*]pyridine derivatives **5**–**21**. (b) Synthesis of 5*H*-indeno[1,2-*b*]pyridines **5**–**21** in a stepwise manner. Reagents and conditions: (i) Toluene, $AcONH_4$, AcOH, Δ, 5 h; (ii) EtOH, room temperature, 24 h; (iii) toluene, $AcONH_4$, AcOH, Δ, 12 h

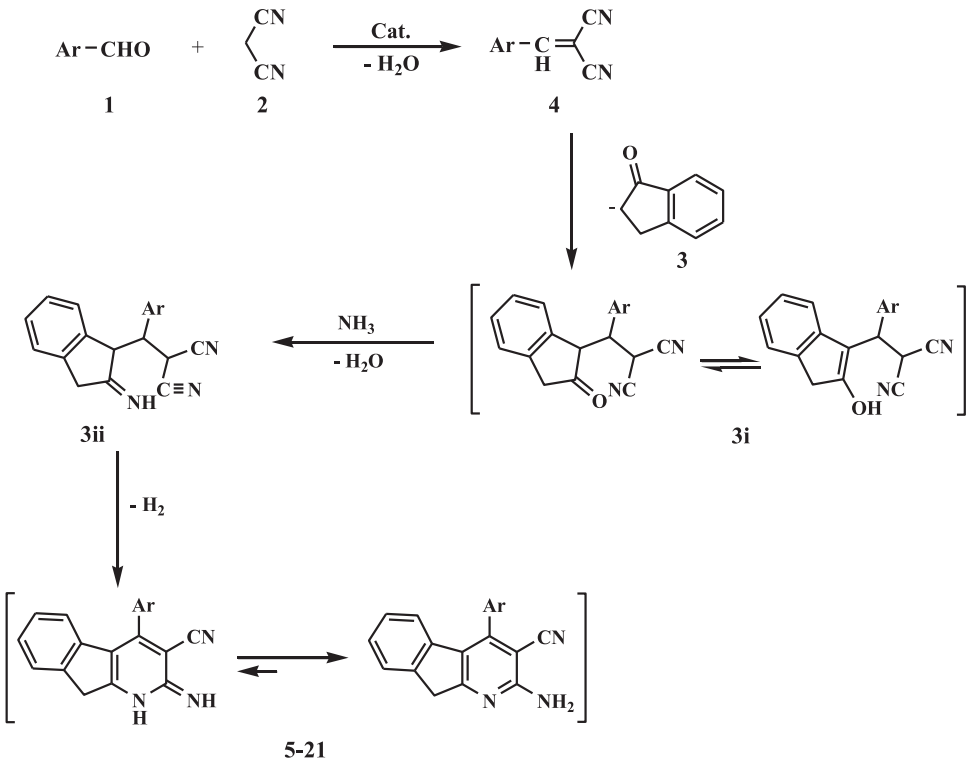

SCHEME 2 A plausible mechanism for the synthesis of compounds **5–21**

TABLE 1 Various substitutions, yield, and melting point data of synthesized derivatives **5–21**

Compound no.	Ar	R_1	R_2	R_3	R_4	Yield %[b]	Yield %[a]	m.p. (°C)
5	3-OCH_3-4OH-C_6H_3	H	H	H	H	78	91	228–230
6	3-OCH_3-4-OH-C_6H_3	H	H	H	OCH_3	74	93	304–306
7	3-OCH_3-4-OH-C_6H_3	H	OCH_3	H	H	70	92	286–288
8	3-OCH_3-4-OH-C_6H_3	OCH_3	H	H	H	67	88	272–274
9	3-OCH_3-4-OH-C_6H_3	H	OCH_3	OCH_3	H	74	90	300–302
10	3-OCH_3-4-OH-C_6H_3	OCH_3	OCH_3	H	H	67	83	276–278
11	(3,4,5-OCH_3)-C_6H_2	H	H	H	H	74	90	288–290
12	(3,4,5-OCH_3)-C_6H_2	H	H	H	OCH_3	74	87	258–260
13	(3,4,5-OCH_3)-C_6H_2	H	OCH_3	OCH_3	H	73	84	278–280
14	(3,4,5-OCH_3)-C_6H_2	OCH_3	OCH_3	H	H	78	85	262–264
15	(3,5-OCH_3)-4-OH-C_6H_2	H	H	H	H	65	86	>310
16	(3,5-OCH_3)-4-OH-C_6H_2	H	OCH_3	OCH_3	H	72	89	>310
17	(3,5-OCH_3)-4-OH-C_6H_2	OCH_3	OCH_3	H	H	68	79	246–248
18	(3,4-OCH_3)-C_6H_3	H	H	H	OCH_3	83	92	218–220
19	(3,4-OCH_3)-C_6H_3	H	OCH_3	OCH_3	H	77	83	234–236
20	(2,4-OCH_3)-C_6H_3	H	OCH_3	OCH_3	H	72	89	240–242
21	4-OCH_3-3-OH-C_6H_3	OCH_3	OCH_3	H	H	75	84	272–274

[a]Three-component process yield % for compounds **5–21**.

[b]Stepwise yield % for compounds **5–21**.

protons of the indeno and aldehydic moiety are reported according to the substitution pattern, respectively, whereas two protons of $-NH_2$ group appear as a broad singlet (brs) between 5.20 and 6.90 ppm in each compound. The ^{13}C NMR spectrum of the same compounds exhibits signals between 31 and 39 ppm, assigned to C5, between 85 and 88 ppm, assigned to C–CN, and at 118 ppm, assigned to –CN, which were also confirmed by DEPT 135°, HETCOR, and FLOCK experiments (see the Supporting Information). The analytical data for all compounds are summarized in Section 4.

To compare the effect of multicomponent strategy on the reaction yield, it was considered worthwhile to attempt the synthesis of **5**–**21** in a stepwise manner (Scheme 1b).

The 2-arylidenemalononitile derivatives **4a**–**f** were achieved according to published procedures[29–32] (see the Supporting Information), and the addition of 1-indanone respective **3** in the presence of ammonium acetate and catalytic amount of acetic acid in toluene at reflux temperature yielded the 5*H*-indeno[1,2-*b*]pyridines **5**–**21**. The results reveal that there was a considerable improvement in the yields obtained when the multicomponent strategy was used (see Table 1). The products were identified by spectra data, and the structures were further confirmed by comparison with data obtained previously.

2.2 | Biological evaluation

2.2.1 | Effect on cell viability and cell growth of derivatives **5**–**21**

The synthesized 5*H*-indeno[1,2-*b*]pyridine derivatives **5**–**21** were tested for their ability to inhibit the viability of human and murine PCa cell lines: advanced androgen-independent bone metastasis prostate cancer (PC-3), androgen-sensitive human prostate adenocarcinoma cells derived from the left supraclavicular lymph node metastasis (LNCaP), and prostate tumor cells derived from rats (MatLyLu). From a total of 17 compounds, 7 were cytotoxic (IC_{50} <200 μM), inhibiting PC-3, LNCaP, and MatLyLu cell viability, and the most active compound **10** was also active against nontumor prostate cells, benign hyperplastic prostatic epithelial cells (BPH-1); however, it showed a more specific response to tumor cells than dequalinium, a drug used as a reference.[33,34] The results are summarized in Table 2.

The effect of compound **10** on cell viability showed a dose-dependent response in all the cell lines tested with inhibition in viability from 15 μM onward. The activity of this compound concentration also followed a time-dependent manner at its cytotoxic IC_{50} (Figure 1).

2.2.2 | Effect, in vitro, on adhesion, propagation, migration, and invasion of PCa cells after exposure to compound **10**

The effect of compound **10** on cell attachment and spreading at their cytotoxic IC_{50} concentration is shown in Figure 2. These results clearly demonstrated the extent of cell attachment and spreading at an incubation period of 0–3 h, showing that compound **10** is an inhibitor of cell adhesion. The measurements were performed on the real-time analyzer xCELLigence.

The wound-healing assay was used to examine the effect of compound **10** on the migration properties of the tumor cells.[35] Compound-free cultures of PC-3 cell line used as controls largely displayed wound recovery within 24 h and cells migrated to the wound (Figure 3). As shown in Figure 4, compound **10** after 18-h incubation period also significantly decreases the invasion of LNCaP cell line using the Boyden chamber coated with Matrigel.

TABLE 2 The antiproliferative activity of compounds **5**–**21** (μM) against PC-3, LNCaP, MatLyLu, and BPH-1 cell lines

Compound no.	PC-3	LNCaP	MatLyLu	BPH-1
9	119.16 ± 1.54	136.94 ± 1.18	131.26 ± 0.77	201.59 ± 1.63
10	45.25 ± 0.23**	18.35 ± 0.08**	26.24 ± 1.13**	92.87 ± 0.15
13	111.39 ± 0.04	196.39 ± 0.28	>250	>250
14	58.56 ± 1.39*	111.18 ± 0.05	>50 ± 1.37	85.77 ± 0.27
16	88.75 ± 0.47	67.11 ± 0.93	>250	185.04 ± 1.51
17	56.78 ± 1.23**	60.10 ± 0.11**	40.08 ± 0.03**	58.98 ± 0.17
21	66.30 ± 0.17**	37.01 ± 1.97**	31.66 ± 1.75**	122.63 ± 1.29
DQA	46.62 ± 4.21**	9.36 ± 1.25**	>50	19.58 ± 4.11

Note: For **5**–**8**, **11**, **12**, **15**, **18**–**20** IC_{50} >200 (μM). Results are expressed as the mean ± *SEM* of the half-maximal inhibitory concentration or IC_{50} (μM). Each experiment was performed three times in five different wells.

Abbreviations: BPH-1, benign hyperplastic prostatic epithelial cells; DQA, dequalinium; LNCaP, androgen-sensitive human prostate adenocarcinoma cells derived from the left supraclavicular lymph node metastasis; MatLyLu, prostate tumor cells derived from rats; PC-3, advanced androgen-independent bone metastasis prostate cancer.

*$p < .05$.

**$p < .001$ compared with BPH-1 cells treated with the compounds.

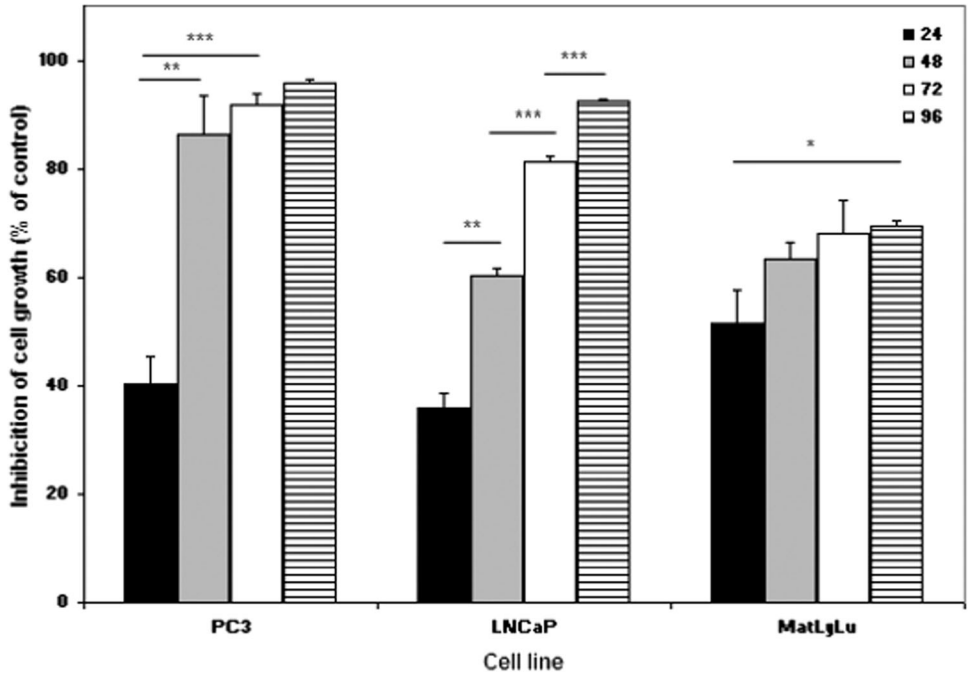

FIGURE 1 Time–response effects of compound **10** at its cytotoxic IC_{50} (Table 2) concentration on PC-3, LNCaP, and MatLyLu cell growth. Results are expressed as the mean ± *SEM*. $^{*}p < .05$; $^{**}p < .01$; and $^{***}p < .001$

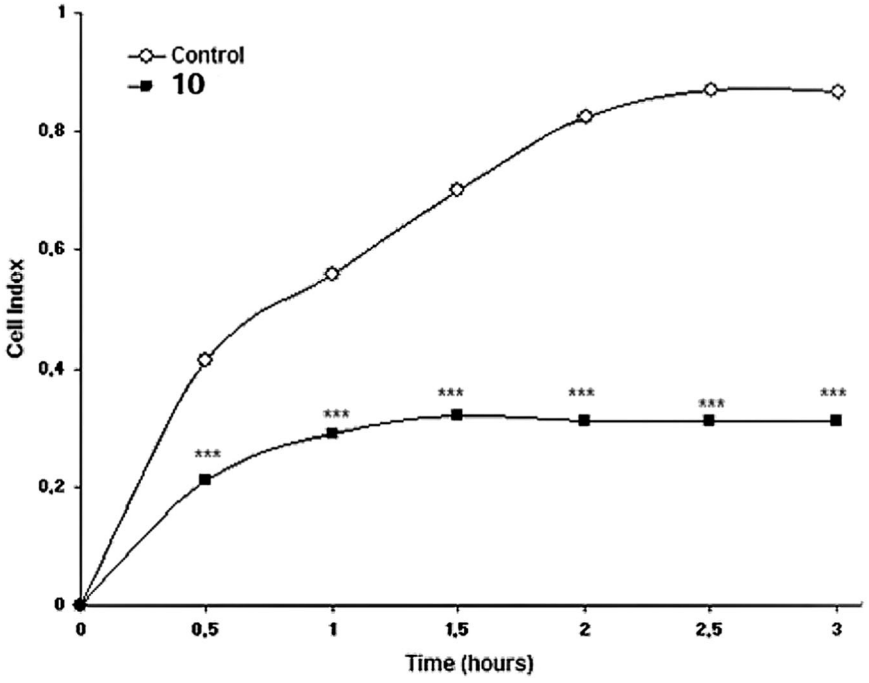

FIGURE 2 Effect of compound **10** on cell adhesion and spreading. PC-3 cells were incubated with the compound at its cytotoxic IC_{50} (Table 2). The cells were applied in triplicate to the fibronectin-coated sensors, and their attachment and spreading were quantified by real-time cell electronic sensing as cell index values (CI) after treatments. Medium–dimethyl sulfoxide (0.2%) alone served as the control (vehicle). The results represent the mean ± *SEM* of three independent experiments.
$^{***}p < .01$ compared with control vehicle

2.2.3 | Inhibition of the activity of MMP-9 against PCa cell lines for compound **10**

MMP-2 and MMP-9 are the two major gelatinases expressed in PCa cells.[24,36] We hypothesized that inhibited migration and invasion of PC-3 and LNCaP cell lines may be originated from the inhibition of those MMPs. The result shows the stronger effect of compound **10** inhibiting the activity of MMP-9 in PC-3 and LNCaP cell lines (Figure 5a,b). We could not detect any MMP-2 activity in both cell lines tested, and gelatin zymography was used to observe activities.

2.2.4 | Effect on colony formation for compound **10**

The ability of PC-3 and LNCaP cell lines to grow in a semi-soft agar medium was examined, using the anchorage-independent growth in

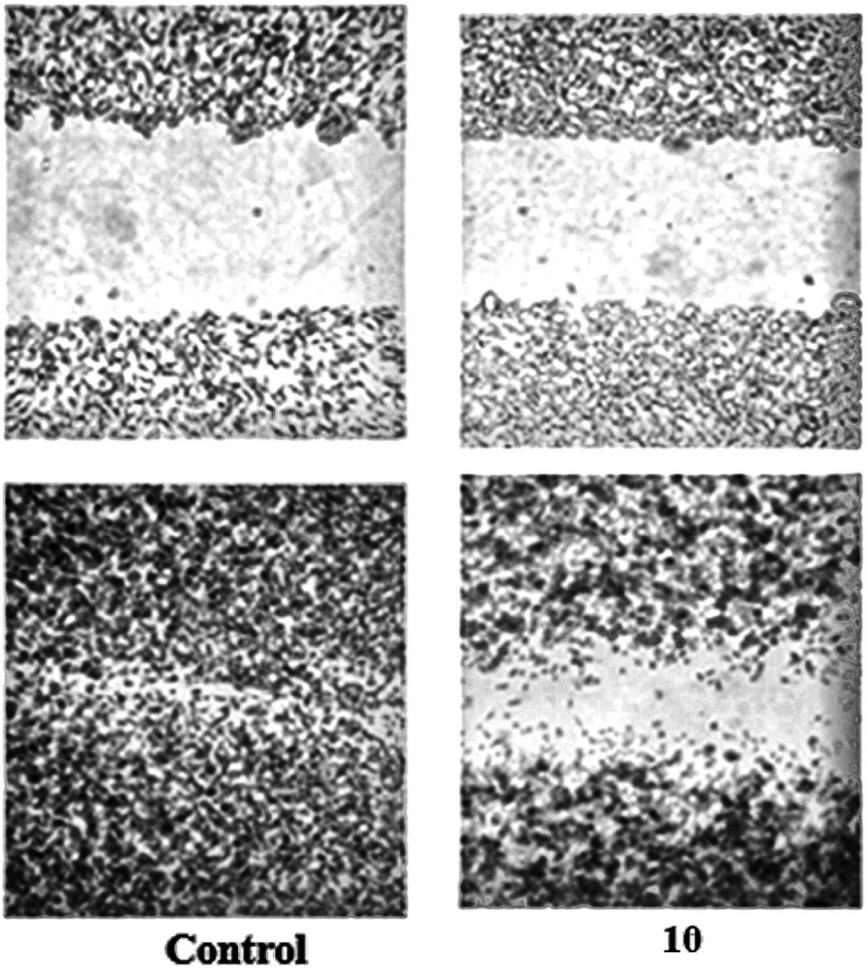

FIGURE 3 Effect of compound **10** on PC-3 wound closure in a single scrape wound model; cells were incubated with the compound at its cytotoxic IC_{50} (Table 2). Representative images of PC-3 cells were captured at the time of wounding and 24 h after that to illustrate recovery from a scrape wound. The images presented are from a representative experiment carried out independently three times

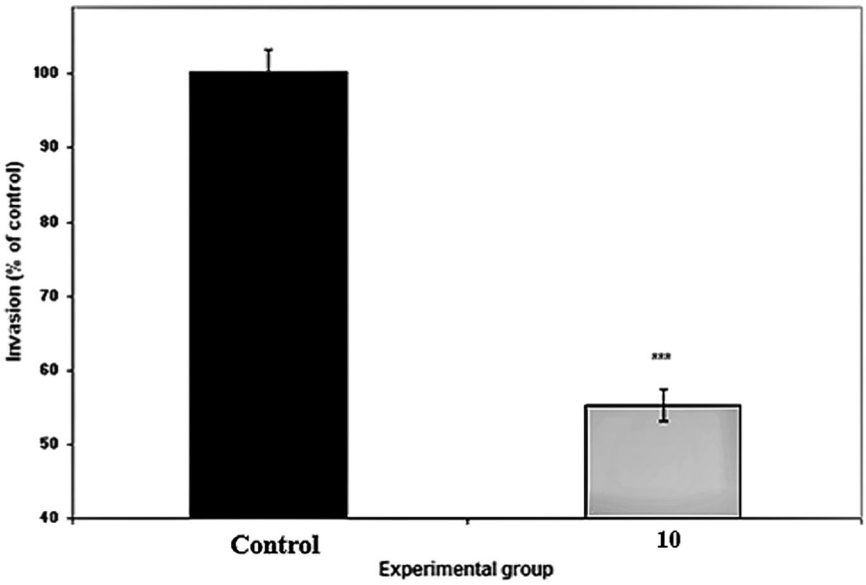

FIGURE 4 Effect of compound **10** on the invasion of LNCaP cells. LNCaP cells were incubated with the compound at its cytotoxic IC_{50} (Table 2). Cells treated with compound **10** or the vehicle were seeded on a Matrigel-coated 0.8-μm porous membrane for 18 h, and the inhibition of invasion, relative to the control vehicle-treated cells, was determined. The results represent the mean ± *SEM* of three independent experiments. $^{***}p < .01$ compared with control vehicle

vitro that correlates with tumorigenesis in nude mice.[37] Cells treated with compound **10** showed a significant decrease in the number and size of the colonies (Figure 6a,b). A significant growth in colonies formed in soft agar was shown by the control vehicle on Day 14 of the incubation period, as previously reported by others.[38]

2.2.5 | Toxicity of compound **10** on brine shrimps

The brine shrimp toxicity bioassay was used to determine the toxicity of compound **10**.[39] The results show that **10** was less toxic to brine shrimps as compared with PC-3, LNCaP, and MatLyLu tumor

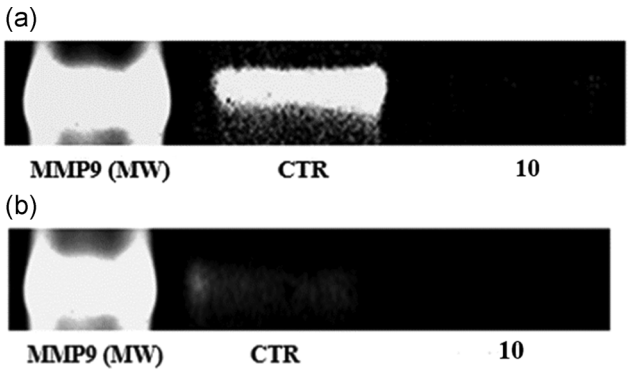

FIGURE 5 Activity of MMP-9 metalloproteinase by gelatin zymography in PC-3 (a) and in LNCaP cells (b) when exposed to compound **10** for 24 h. Cell lines were incubated with the compound at its cytotoxic IC_{50} (Table 2). Conditioned medium prepared from subconfluent cultures was collected, resolved in nonreducing gels containing gelatin (1 mg/ml), and processed for zones of gel degradation activity. Only the results in PC-3 cells were quantified in relation to control vehicle and are presented as the mean ± *SEM* of the percentage of activity in three different experiments (b). ***$p < .001$ compared with control vehicle

cell lines (Table 3). The toxicity-to-antitumor ratio (TAR) was used to confirm the lower toxicological effect of compound **10**. The TAR is defined as the ratio of the LC_{50} concentration in the brine shrimp assay to the IC_{50} antitumor cytotoxicity concentration, which was always higher than 1; thus, the tumor cells were more sensitive to compound **10**.

TABLE 3 Toxicological effect of compound **10** on brine shrimp

Compound no.	LC_{50} (μM)	TAR PC-3	TAR LNCaP	TAR MatLyLu
10	302.12 ± 1.93	6.7	16.5	11.5

Note: The toxicological effect was tested by the brine shrimp bioassay. LC_{50} represents the half lethal concentration in the brine shrimp assay, respectively. The toxicity-to-antitumor ratio (TAR) is defined by the value resulted of the LC_{50} divided by the IC_{50} values (Table 2) of the corresponding compound for PC-3, LNCaP, or MatLyuLu cell lines.

3 | CONCLUSION

In summary, our study describes the synthesis of *2*-amino-4-(phenylsubstituted)-5*H*-indeno[1,2-*b*]pyridine-3-carbonitrile derivatives through sequential multicomponent reaction of aromatic aldehydes, malononitrile, and 1-indanones, as well as their anticancer evaluation. The effect of one-pot method in the generation of the target product has been studied by thin-layer chromatography, IR, ^{1}H NMR, ^{13}C NMR, DEPT 130°, HETCOR, FLOCK. However, the biological study showed that compound **10** significantly impeded the proliferation of PC-3, LNCaP, and MatLyLu cell lines. The antimetastatic effects of **10** could be related with the inhibition of MMP9 in PC-3 and LNCaP human cell lines; these results coincide with the results previously reported for analog molecules.[11,24,40]

A study of the structure–activity relationship of these compounds allows us to propose that the presence of two methoxy groups at positions 6, 7 of the indeno nucleus and a

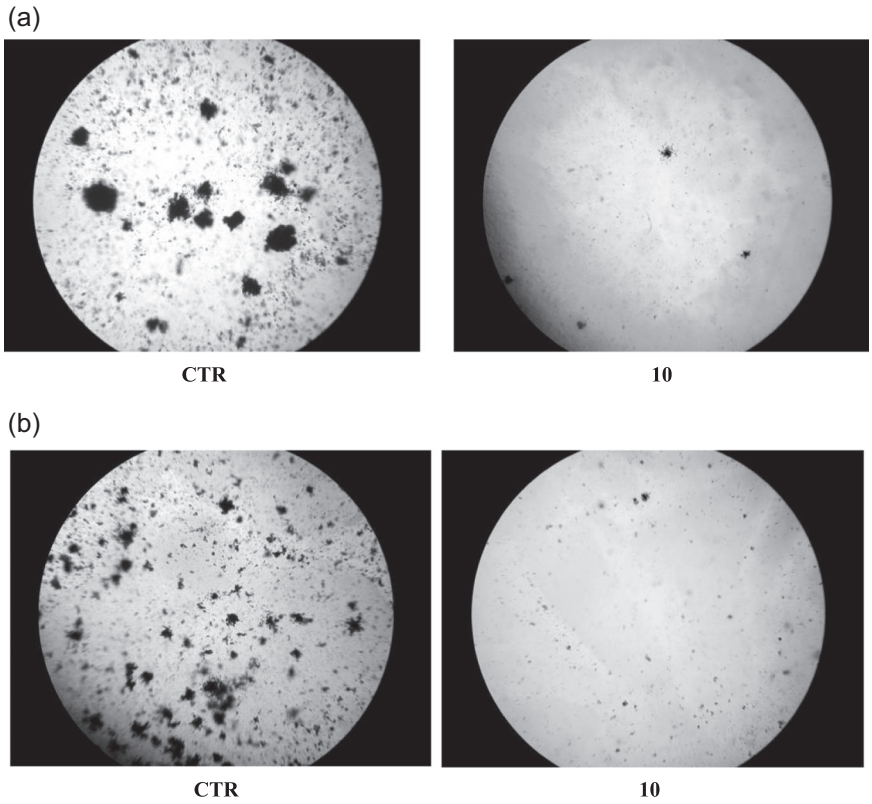

FIGURE 6 Effect of compound **10** at its cytotoxic IC_{50} (Table 2) on the formation of colonies in soft agar. PC-3 (a) and LNCaP cells (b) were plated over a semi-solid layer of soft agar treated with the compound and incubated for 14 days. The results represent standard images of three different experiments

4-hydroxy-3-methoxy phenyl substitution pattern at position 4 of the pyridine ring is decisive for these types of molecules to exert a very good antiproliferative activity. The activity is affected when the substitution pattern in the phenyl group at position 4 of pyridine changes to 3-hydroxy-4-methoxy, compound **21**, and is marginalized when another methoxy group is introduced at position 5. Other substitution patterns with these same groups in both the indeno ring and the phenyl ring significantly affect the antiproliferative activity of these types of compounds. This study shows the importance of 5*H*-indeno[1,2-*b*]pyridine derivatives as potential anticancer agents, to improve PC chemotherapy by inhibiting the metastasis process. Other studies will be required to explore an exact mechanism of action that allows us to clarify the roles of functional groups in anticancer activity in this type of nucleus.

4 | EXPERIMENTAL

4.1 | Chemistry

4.1.1 | General

Thin-layer chromatography was carried out on Merck silica F_{254} 0.255-mm plates, and spots were visualized by UV fluorescence at 254 nm. Elemental analyses were performed using a PerkinElmer 2400 CHN elemental analyzer. The results were within ±0.4% of the predicted values. NMR spectra were obtained using a JEOL Eclipse™ at 270 MHz for ^{1}H NMR and at 67.9 MHz for ^{13}C NMR using $CDCl_3$ or DMSO-d_6, and are reported in ppm downfield from the residual $CHCl_3$ or DMSO (δ 7.25 or 2.50 for ^{1}H NMR and 77.0 or 39.8 for ^{13}C NMR, respectively) (see the Supporting Information for the original spectra). A Nicolet™ IS5 FT-IR (ID3 Zn-Se) spectrophotometer was used to determine the IR spectra. A Thomas micro hot-stage device was used to determine the melting points (mp). All organic products or solvents (from Sigma-Aldrich Group) were used directly or distilled and dried in the usual manner, respectively.

The InChI codes of the investigated compounds, together with some biological data, are provided as Supporting Information.

4.1.2 | General procedure for the synthesis of 2-amino-4-(phenylsubstituted)-5*H*-indeno[1,2-*b*]-pyridine-3-carbonitrile **5–21**

Benzaldehyde-substituted **1** (1 mmol), malononitrile **2** (1 mmol), 1-indanone **3** (1 mmol), and ammonium acetate (1.5 mmol), in 10 ml of toluene, with catalytic amount of acetic acid, were combined in a 20-ml round-bottom flask fitted with a reflux condenser and Dean–Stark trap. The mixture was heated under reflux for 5 h and the solvent was then evaporated using a rotary evaporator. The residue was then poured into crushed ice. The desired product was isolated, filtered, and washed with cold water–ethanol (1:1). The solid was recrystallized from ethanol.

*2-Amino-4-(4′-hydroxy-3′-methoxyphenyl)-5H-indeno[1,2-b]-pyridine-3-carbonitrile (**5**)*

IR KBr (cm^{-1}): 3372, 3326, 2205, 1554, 1510; ^{1}H NMR ($CDCl_3$) δ ppm: 3.85 (s, 2H, H_5), 3.95 (s, 3H, OCH_3), 5.83 (s, 2H, OH), 7.04–7.08 (m, 3H, Ar–H), 7.36–7.52 (m, 4H, Ar–H), 8.40 (brs, 2H, NH_2); ^{13}C NMR (DMSO-d_6) δ ppm: 39.5, 56.50, 113.3, 116.2, 120.8, 121.9, 125.9, 127.6, 127.9, 128.8, 133.9, 141.3, 143.8, 144.9, 147.4, 148.3; anal. calcd. for $C_{20}H_{15}N_3O_2$: % C, 72.94; H, 4.59; N, 12.76. Found: % C, 73.01; H, 4.63; N, 12.95.

*2-Amino-9-methoxy-4-(4′-hydroxy-3′-methoxyphenyl)-5H-indeno-[1,2-b]pyridine-3-carbonitrile (**6**)*

IR KBr (cm^{-1}): 3356, 3312, 2224, 1593, 1555; ^{1}H NMR (DMSO-d_6) δ ppm: 3.74 (s, 2H, H_5), 3.83 (s, 3H, OCH_3), 3.92 (s, 3H, OCH_3), 6.60 (s, 2H, NH_2), 6.92 (d, 1H, $H_{5'}$, J = 8.2 Hz), 7.01–7.05 (m, 2H, Ar–H), 7.14–7.18 (m, 2H, Ar–H), 7.38 (t, 1H, H_7, J = 7.9 Hz), 9.42 (s, 1H, OH); ^{13}C NMR (DMSO-d_6) δ ppm: 34.0, 56.2, 56.4, 85.8, 110.6, 113.4, 116.1, 118.1, 118.6, 122.2, 123.6, 127.1, 127.7, 131.6, 148.0, 148.1, 148.9, 149.6, 157.0, 162.0, 162.8; anal. calcd. for $C_{21}H_{17}N_3O_3$: % C, 70.18; H, 4.77; N, 11.69. Found: % C, 70.19; H, 4.77; N, 11.81.

*2-Amino-7-methoxy-4-(4′-hydroxy-3′-methoxyphenyl)-5H-indeno-[1,2-b]pyridine-3-carbonitrile (**7**)*

IR KBr (cm^{-1}): 3376, 3299, 2208, 1600, 1561; ^{1}H NMR (DMSO-d_6) δ ppm: 3.73 (s, 2H, H_5), 3.83 (s, 6H, OCH_3), 6.75 (brs, 2H, NH_2), 6.91 (d, 1H, $H_{5'}$, J = 8.2 Hz), 7.01–7.07 (m, 2H, Ar–H), 7.17–7.20 (m, 2H, Ar–H), 7.76 (d, 1H, H_9, J = 8.4 Hz), 9.46 (s, 1H, OH); ^{13}C NMR (DMSO-d_6) δ ppm: 33.9, 56.0, 56.4, 85.6, 110.9, 113.4, 114.7, 116.1, 118.7, 122.2, 122.9, 123.3, 127.1, 133.0, 148.0, 148.1, 148.9, 148.9, 150.1, 162.4, 162.6; anal. calcd. for $C_{21}H_{17}N_3O_3$: % C, 70.18; H, 4.77; N 11.69. Found: % C, 70.25; H, 4.83; N, 11.89.

*2-Amino-6-methoxy-4-(4′-hydroxy-3′-methoxyphenyl)-5H-indeno-[1,2-b]pyridine-3-carbonitrile (**8**)*

IR KBr (cm^{-1}): 3378, 3312, 2210, 1558, 1507; ^{1}H NMR (DMSO-d_6) δ ppm: 3.73 (s, 2H, H_5), 3.87 (s, 6H, OCH_3), 6.96–7.06 (m, 4H, Ar–H, NH_2), 7.20 (dd, 1H, $H_{6'}$, J_1 = 1.7 Hz, J_2 = 8.0 Hz), 7.34 (d, 1H, $H_{2'}$, J = 1.7 Hz), 7.4 (t, 1H, H_8, J_1 = 7.4 Hz), 7.67 (d, 1H, H_9, J = 7.4 Hz), 9.33 (s, 1H, OH); ^{13}C NMR (DMSO-d_6) δ ppm: 31.8, 55.8, 56.6, 85.8, 110.9, 110.9, 111.1, 113.4, 113.5, 116.2, 116.9, 118.6, 122.1, 129.5, 131.7, 133.8, 142.8, 148.3, 156.5, 161.9, 162.7; anal. calcd. for $C_{21}H_{17}N_3O_3$: % C, 70.18; H, 4.77; N, 11.69. Found: % C, 70.22; H, 4.79; N, 11.91.

*2-Amino-7,8-dimethoxy-4-(4′-hydroxy-3′-methoxyphenyl)-5H-indeno[1,2-b]pyridine-3-carbonitrile (**9**)*

IR KBr (cm^{-1}): 3374, 3340, 2215, 1605, 1504; ^{1}H NMR (DMSO-d_6) δ ppm: 3.66 (s, 2H, H_5), 3.82 (s, 6H, OCH_3), 3.83 (s, 3H, OCH_3), 6.72 (brs, 2H, NH_2), 6.91 (d, 1H, $H_{5'}$, J = 8.2 Hz), 7.03 (dd, 1H, $H_{6'}$, J_1 = 1.9 Hz, J_2 = 8.2 Hz), 7.19 (d, 1H, $H_{2'}$, J = 1.9 Hz), 7.22 (s, 1H, H_6), 7.31 (s, 1H, H_9), 9.46 (s, 1H, OH); ^{13}C NMR (DMSO-d_6) δ ppm: 34.5, 56.1, 56.3, 56.4, 85.2, 103.8, 109.0, 113.4, 116.0, 118.8, 122.2, 123.8, 127.1, 132.4, 140.2, 147.9, 148.1, 149.4, 151.7, 162.4, 163.1; anal.

calcd. for $C_{22}H_{19}N_3O_4$: % C, 67.86; H, 4.92; N, 10.79. Found: % C, 67.86; H, 4.94; N, 10.93.

*2-Amino-6,7-dimethoxy-4-(4′-hydroxy-3′-methoxyphenyl)-5H-indeno[1,2-b]pyridine-3-carbonitrile (**10**)*

IR KBr (cm^{-1}): 3356, 3344, 2211, 1603, 1555; ^1H NMR (DMSO-d_6) δ ppm: 3.35 (s, 2H, H_5), 3.79 (s, 3H, OCH_3), 3.81 (s, 3H, OCH_3), 3.83 (s, 3H, OCH_3), 6.75 (brs, 2H, NH_2), 6.93 (d, 1H, $H_{5'}$, J = 8.0 Hz), 7.03 (dd, 1H, $H_{6'}$, J_1 = 1.0 Hz, J_2 = 8.0 Hz), 7.18 (m, 2H, $H_{2',6}$), 7.57 (d, 1H, H_9, J = 8.4 Hz), 9.46 (s, 1H, OH); ^{13}C NMR (DMSO-d_6) δ ppm: 31.0, 56.4, 56.6, 60.3, 85.9, 113.4, 113.4, 116.1, 117.7, 122.2, 123.3, 126.9, 134.1, 138.7, 145.6, 148.0, 148.2, 150.5, 154.1, 162.3, 162.4; anal. calcd. for $C_{22}H_{19}N_3O_4$: % C, 67.86; H, 4.92; N, 10.79. Found: % C, 67.90; H, 4.97; N, 10.89.

*2-Amino-4-(3′,4′,5′-trimethoxyphenyl)-5H-indeno[1,2-b]pyridine-3-carbonitrile (**11**)*

IR KBr (cm^{-1}): 3343, 3260, 2207, 1638, 1561; ^1H NMR ($CDCl_3$) δ ppm: 3.86 (s, 2H, H_5), 3.94 (s, 3H, OCH_3), 3.99 (s, 6H, OCH_3), 7.03–713 (m, 3H, $H_{2',6'}$, Ar), 7.37–7.53 (m, 3H, Ar–H), 8.41 (brs, 2H, NH_2); ^{13}C NMR (DMSO-d_6) δ ppm: 39.5, 57.0, 61.2, 106.7, 106.9, 121.0, 126.2, 127.9, 129.1, 134.3, 137.9, 141.4, 143.9, 145.2, 147.4, 153.7, 153.9, 159.9; anal. calcd. for $C_{22}H_{19}N_3O_3$: % C, 70.76; H, 5.13; N, 11.25. Found: % C, 70.78; H, 5.17; N, 11.57.

*2-Amino-9-methoxy-4-(3′,4′,5′-trimethoxyphenyl)-5H-indeno[1,2-b]-pyridine-3-carbonitrile (**12**)*

IR KBr (cm^{-1}): 3392, 3312, 2210, 1602, 1494; ^1H NMR (DMSO-d_6) δ ppm: 3.74 (s, 2H, H_5), 3.77 (s, 3H, OCH_3), 3.83 (s, 6H, OCH_3), 3.92 (s, 3H, OCH_3), 6.69 (brs, 2H, NH_2), 6.91 (s, 2H, $H_{2',6'}$), 7.03 (d, 1H, H_6, J = 7.6 Hz), 7.16 (d, 1H, H_8, J = 7.6 Hz), 7.40 (t, 1H, H_7, J = 7.6 Hz); ^{13}C NMR (DMSO-d_6) δ ppm: 33.9, 56.1, 56.7, 60.6, 85.6, 106.7, 110.5, 118.1, 118.4, 123.6, 126.4, 127.6, 131.7, 138.4, 148.9, 149.4, 154.5, 157.0, 161.9, 163.0; anal. calcd. for $C_{23}H_{21}N_3O_4$: % C, 68.47; H, 5.25; N. 10.42. Found: % C, 68.51; H, 5.27; N, 10.61.

*2-Amino-7,8-dimethoxy-4-(3′,4′,5′-trimethoxyphenyl)-5H-indeno-[1,2-b]pyridine-3-carbonitrile (**13**)*

IR KBr (cm^{-1}): 3317, 3290, 2203, 1632, 1552; ^1H NMR (DMSO-d_6) δ ppm: 3.69 (s, 2H, H_5), 3.75 (s, 3H, OCH_3), 3.82 (s, 3H, OCH_3), 3.83 (s, 6H, OCH_3), 3.84 (s, 3H, OCH_3), 6.80 (brs, 2H, NH_2), 6.93 (s, 2H, $H_{2',6'}$), 7.22 (s, 1H, H_6), 7.33 (s, 1H, H_9); ^{13}C NMR (DMSO-d_6) δ ppm: 34.5, 56.0, 56.3, 56.7, 60.7, 85.1, 103.8, 106.8, 108.9, 118.6, 123.9, 131.7, 132.7, 138.4, 140.3, 149.4, 150.2, 151.8, 153.4, 162.3, 163.3; anal. calcd. for $C_{24}H_{23}N_3O_5$: % C, 66.50; H, 5.35; N, 9.69. Found: % C, 66.53; H, 5.38; N, 9.87.

*2-Amino-6,7-dimethoxy-4-(3′,4′,5′-trimethoxyphenyl)-5H-indeno-[1,2-b]pyridine-3-carbonitrile (**14**)*

IR KBr (cm^{-1}): 3324, 3298, 2208, 1615, 1488; ^1H NMR (DMSO-d_6) δ ppm: 3.74 (s, 2H, H_5), 3.76 (s, 3H, OCH_3), 3.79 (s, 3H, OCH_3), 3.83 (s, 6H, OCH_3), 3.88 (s, 3H, OCH_3), 6.91 (brs, 2H, NH_2), 6.99 (s, 2H, $H_{2',6'}$), 7.17 (d, 1H, H_8, J = 8.2 Hz), 7.75 (d, 1H, H_9, J = 8.2 Hz); ^{13}C NMR (DMSO-d_6) δ ppm: 31.8, 56.7, 56.8, 60.3, 60.6, 85.1, 106.5, 113.2, 116.5, 118.6, 132.5, 135.3, 136.9, 143.7, 145.8, 153.0, 153.8, 159.5, 160.1, 162.3; anal. calcd. for $C_{24}H_{23}N_3O_5$: % C, 66.50; H, 5.35; N, 9.69. Found: % C, 66.56; H, 5.41; N, 9.91.

*2-Amino-4-(4′-hydroxy-3′,5′-dimethoxyphenyl)-5H-indeno[1,2-b]-pyridine-3-carbonitrile (**15**)*

IR KBr (cm^{-1}): 3388, 3317, 2219, 1603, 1552; ^1H NMR (DMSO-d_6) δ ppm: 3.86 (s, 3H, OCH_3), 3.87 (s, 2H, H_5), 3.96 (s, 3H, OCH_3), 7.03 (s, 2H, $H_{2',6'}$), 7.41–7.52 (m, 4H, Ar–H, NH_2), 7.60 (d, 1H, H_6, J = 7.2 Hz), 8.10 (d, 1H, H_9, J = 7.2 Hz), 8.66 (s, 1H, OH); ^{13}C NMR (DMSO-d_6) δ ppm: 34.5, 56.6, 56.9, 85.6, 106.8, 118.4, 120.8, 125.9, 127.6, 128.8, 133.9, 141.4, 144.9, 148.8, 152.8, 160.1, 162.0; anal. calcd. for $C_{21}H_{17}N_3O_3$: % C, 70.18; H, 4.77; N, 11.69. Found: % C, 70.24; H, 4.80; N, 11.85.

*2-Amino-7,8-dimethoxy-4-(4′-hydroxy-3′,5′-dimethoxyphenyl)-5H-indeno[1,2-b]pyridine-3-carbonitrile (**16**)*

IR KBr (cm^{-1}): 3392, 3317, 2215, 1616, 1518; ^1H NMR (DMSO-d_6) δ ppm: 3.71 (s, 2H, H_5), 3.81 (s, 6H, OCH_3), 3.82 (s, 3H, OCH_3), 3.84 (s, 3H, OCH_3), 6.73 (s, H, NH_2), 6.89 (s, 2H, $H_{2',6'}$), 7.23 (s, 1H, H_6), 7.32 (s, 1H, H_9), 8.81 (s, 1H, OH); ^{13}C NMR (DMSO-d_6) δ ppm: 34.5, 56.1, 56.3, 56.8, 85.3, 103.8, 107.0, 109.0, 118.8, 123,9, 126.1, 132.4, 137.1, 140.3, 148.4, 149.4, 149.9, 151.7, 162.3, 163.2; anal. calcd. for $C_{23}H_{21}N_3O_5$: % C, 65.86; H, 5.05; N, 10.02. Found: % C, 65.89; H, 5.09; N, 9.97.

*2-Amino-6,7-dimethoxy-4-(4′-hydroxy-3′,5′-dimethoxyphenyl)-5H-indeno[1,2-b]pyridine-3-carbonitrile (**17**)*

IR KBr (cm^{-1}): 3324, 3234, 2215, 1609, 1558; ^1H NMR (DMSO-d_6) δ ppm: 3.76 (s, 2H, H_5), 3.80 (s, 6H, OCH_3), 3.81 (s, 6H, OCH_3), 3.87 (s, 3H, OCH_3), 6.76 (brs, 2H, NH_2), 6.89 (s, 2H, $H_{2',6'}$), 7.19 (d, 1H, H_8, J = 8.2 Hz), 7.58 (d, 1H, H_9, J = 8.2 Hz), 8.81 (brs, 1H, OH); ^{13}C NMR (DMSO-d_6) δ ppm: 31.3, 56.7, 56.9, 60.3, 86.1, 107.0, 113.4, 117.7, 118.6, 123.4, 126.0, 134.1, 137.2, 138.6, 145.6, 148.5, 150.7, 154.1, 162.3, 162.4; anal. calcd. for $C_{23}H_{21}N_3O_5$: % C, 65.86; H, 5.05; N, 10.02. Found: % C, 65.89; H, 5.07; N, 10.27.

*2-Amino-9-methoxy-4-(3′,4′-dimethoxyphenyl)-5H-indeno[1,2-b]-pyridine-3-carbonitrile (**18**)*

IR KBr (cm^{-1}): 3340, 3328, 2208, 1593, 1504; ^1H NMR (DMSO-d_6) δ ppm: 3.73 (s, 2H, H_5), 3.81 (s, 3H, OCH_3), 3.84 (s, 3H, OCH_3), 3.92 (s, 3H, OCH_3), 6.65 (s, 2H, NH_2), 7.04 (d, 1H, $H_{5'}$, J = 8.2 Hz), 7.09–7.19 (m, 4H, Ar–H), 7.42 (t, 1H, H_7, J = 7.8 Hz); ^{13}C NMR (DMSO-d_6) δ ppm: 33.9, 56.1, 56.3, 56.9, 85.7, 103.8, 110.6, 112.2, 112.9, 118.1, 118.4, 121.9, 123.7, 127.5, 128.6, 131.7, 148.9, 149.1, 149.9, 157.0, 161.9, 163.9; anal. calcd. for $C_{22}H_{19}N_3O_3$: % C, 70.76; H, 5.13; N, 11.25. Found: % C, 70.80; H, 5.16; N, 11.42.

*2-Amino-7,8-dimethoxy-4(3′,4′-dimethoxyphenyl)-5H-indeno[1,2-b]-pyridine-3-carbonitrile (**19**)*

IR KBr (cm^{-1}): 3312, 3283, 2212, 1635, 1552; ^1H NMR (DMSO-d_6) δ ppm: 3.67 (s, 2H, H_5), 3.81 (s, 3H, OCH_3), 3.82 (s, 3H, OCH_3), 3.84 (s,

6H, OCH_3), 6.76 (brs, 2H, NH_2), 7.09 (d, 1H, $H_{5'}$, J = 8.2 Hz), 7.15 (dd, 1H, J_1 = 1.1 Hz, J_2 = 8.2 Hz $H_{6'}$), 7.22 (s, 2H, $H_{2',6}$), 7.32 (s, 1H, H_9); ^{13}C NMR (DMSO-d_6) δ ppm: 31.3, 56.1, 56.3, 56.6, 57.2, 85.2, 103.8, 108.9, 112.2, 112.8, 118.7, 121.9, 123.9, 128.6, 132.3, 140.2, 149.1, 149.4, 149.9, 162.3, 163.2; anal. calcd. for $C_{23}H_{21}N_3O_4$: % C, 68.47; H, 5.25; N, 10.42. Found: % C, 68.48; H, 5.26; N, 10.57.

*2-Amino-7,8-dimethoxy-4(2′,4′-dimethoxyphenyl)-5H-indeno[1,2-b]-pyridine-3-carbonitrile (**20**)*

IR KBr (cm^{-1}): 3372, 3296, 2208, 1596, 1571; ^{1}H NMR (DMSO-d_6) δ ppm: 3.77 (s, 2H, H_5), 3.81 (s, 3H, OCH_3), 3.84 (s, 3H, OCH_3), 3.85 (s, 6H, OCH_3), 6.64–6.68 (m, 3H, $H_{5'}$, NH_2), 6.72 (d, 1H, $H_{3'}$, J = 2.2 Hz), 7.18 (s, 1H, H_6), 7.26 (d, 1H, $H_{6'}$, J = 8.40 Hz), 7.30 (s, 1H, H_9); ^{13}C NMR (DMSO-d_6) δ ppm: 31.3, 55.9, 56.1, 56.3, 87.1, 99.4, 103.8, 105.9, 109.1, 117.4, 118.3, 125.2, 131.3, 132.4, 139.8, 147.2, 149.5, 151.6, 157.8, 161.8, 161.9, 162.8; anal. calcd. for $C_{23}H_{21}N_3O_4$: % C, 68.47; H, 5.25; N, 10.42. Found: % C, 68.51; H, 5.29; N, 10.61.

*2-Amino-6,7-dimethoxy-4-(3-hydroxy-4-methoxyphenyl)-5H-indeno-[1,2-b]pyridine-3-carbonitrile (**21**)*

IR KBr (cm^{-1}): 3376, 2208, 1616, 1555, 1497; ^{1}H NMR (DMSO-d_6) δ (ppm): 3.59 (s, 2H, H_5), 3.82 (s, 3H, OCH_3), 3.84 (s, 3H, OCH_3), 3.85 (s, 3H, OCH_3), 6.76 (brs, 2H, NH_2), 7.02–7.09 (m, 3H, $H_{2',5',6'}$), 7.21 (d, 1H, H_8, J = 8.2 Hz), 7.28 (d, 1H, H_9, J = 8.2 Hz), 9.32 (s, 1H, OH); ^{13}C NMR (DMSO-d_6) δ (ppm): 33.6, 56.1, 56.3, 56.7, 86.1, 103.8, 108.9, 112.6, 116.3, 118.7, 120.4, 123.6, 128.7, 132.3, 140.1, 146.9, 148.9, 149.5, 151.6, 162.2, 163.0; anal. calcd. for $C_{22}H_{19}N_3O_4$: % C, 67.86; H, 4.92; N, 10.79. Found: % C, 67.88; H, 4.95; N, 11.01.

4.2 | Biology

4.2.1 | Effect of compounds **5**–**21** on cell viability and cell growth

A 96-well microtiter plate (tissue culture grade) containing 0.1 ml of growth medium/well (RPMI) was seeded with PC-3 (5×10^3), LNCaP (1.2×10^4), or MatLyLu (5×10^2) prostate tumor cell lines. The cells were exposed after 24 h of culture to the cytotoxic action of compounds **5**–**21** dissolved in dimethylsulfoxide (DMSO) for 72 h at concentrations ranging from 15 to 250 µM. The final concentration of DMSO in the culture medium was always lower than 0.2%.

After the incubation time, cells were incubated with sodium 3-[1-(phenylaminocarbonyl)-3,4-tetrazolium]-bis(4-methoxy-6-nitro) benzene sulfonic acid hydrate (XTT)[11,41] at 37°C for 4 h, and the colorimetric detection of the orange product formazan was registered at 492 nm (Tecan SpectraFluor). The cytotoxic IC_{50} value obtained with the XTT assay was defined as the concentration of tested compounds resulting in a 50% reduction of viability as compared with vehicle-treated cells. The experiments were carried out in triplicates. The most active compound was chosen for further procedures using the IC_{50} values obtained by this evaluation.

The time-dependent effects of the best compound on cell growth were measured according to a previous procedure described.[42] The PC-3 (1×10^5), LNCaP (2.4×10^5), or MatLyLu (1.5×10^4) cell lines were seeded in six-well plates in RPMI containing 10% fetal bovine serum (FBS) and the compound at its cytotoxic IC_{50} (37°C, 95% O_2, 5% CO_2). Cells were collected from culture dishes after trypsin–EDTA treatment for 7 min at 37°C. A hemocytometer was used for counting the number of viable cells at 24 h intervals for a period of 96 h.

4.2.2 | Cell adhesion assay

An xCELLigence Real-Time Cell Analyzer from Applied Science Roche was used to perform measurements. The system monitors the biological status of cells as cell number and adhesion by measuring electrical impedance via microelectrodes fixed at the bottom of special 96-well tissue plates. The analyzer automatically measures the electrical impedance as cell index (CI), which is transferred, analyzed, and processed by the integrated software.[43] Under the same physiological conditions, a larger impedance would result in a larger CI number, a consequence that more cells have been attached to the electrodes in the plate. Results are expressed as CI and relative attachment and spreading. For the measurements, the special 96-well ACEA E-plates® were coated with fibronectin (20 µg/ml), 1 h at 37°C. With a phosphate-buffered saline (PBS), the plates were washed and coated with bovine serum albumin solution in PBS (0.5%) for 20 min at 37°C, after which each well was washed with PBS. Next, 50 µl of the medium was added to record the background, and then 100 µl of PC-3 cell suspension (5×10^5 cells) was transferred to each well of the ACEA E-plates® and 50 µl of the most active compound **10** at its cytotoxic IC_{50} (Table 2) was added. The spreading and adhesion of the cells were monitored every minute using this real-time cell electronic sensing system according to the manufacturer's instructions for a period up to 4 h.[22,35]

4.2.3 | Cell migration and invasion evaluation

Cell migration was determined by the scraping wound repair test.[35] 8×10^4 PC-3 cells were grown to confluence on 24-well plates (48 h, 37°C). The sterilized micropipette tip was used to produce a wound throughout the entire cell monolayer and then the medium was disposed of. After being washed with PBS, compound **10** at its cytotoxic IC_{50} (Table 2) was added in a newly prepared medium and, in the presence of endothelial growth factor (1 pg/ml), was incubated for 24 h. Coverslips were placed in a light microscope, and the images of the wounds were captured through a computer system using a digital camera immediately after wounding (0 h) and after 24 h of incubation. The results were expressed as percentage of wound closure and the number of migrated cells/mm^2.

LNCaP human tumor cells (1×10^5 cells/ml) were used for cell invasion test; these were pretreated with compound **10** at its

cytotoxic IC_{50} for 24 h. After this time, the cells were seeded at the top of the Boyden chamber (Matrigel-coated membrane) in 50 µl of serum-free media and incubated for 18 h at 37°C. The bottom of the chamber contained 500 µl of standard medium with 20% FBS. The cells that had invaded into the lower surface of the chamber were reacted with calcein (4 µg/ml) in Hank's Buffered Salt Solution (HBSS) for 1 h at 37°C. The fluorescence generated by the cells was read at 485/530 nm.[11,22]

4.2.4 | MMP zymography

The gelatinolytic activities of MMP-2 and MMP-9 were assayed by electrophoresis on 10% polyacrylamide gels containing 1 mg/ml gelatin in the conditioned culture medium.[44] In brief, PC-3 and LNCaP cells (80% confluent in six-well plates) were washed twice with PBS and treated with the most active compound at its cytotoxic IC_{50} (Table 2) in 2.5 ml of serum-free medium using the following conditions: 24 h at 37°C in a humidified atmosphere of 95% O_2 and 5% CO_2. Then, 20 µl of a mixture composed of the conditioned medium and sample buffer (without β-mercaptoethanol, 0.75:0.25) was subjected to electrophoresis on 10% sodium dodecyl sulfate (SDS)–polyacrylamide gel electrophoresis copolymerized with 1 mg/ml of gelatin as a substrate. After electrophoresis was completed at 100 V, to remove SDS, the gel was washed with a 2% solution of Triton X-100 and incubated for 20 h at 37°C in a buffer made up of 50 mM Tris-HCl, pH 7.4, 0.2 mM NaCl, 10 mM $CaCl_2$. Gels were then dyed with 0.5% Coomassie brilliant blue and subsequently faded in water–methanol–acetic acid (50:40:10). Undyed regions of the gel corresponding to gelatinase activity were quantified using ImageJ software for Windows. As a positive control, pure human proteins MMP-2 and MMP-9 were used.[11,22]

4.2.5 | Measurement of clonogenic potential

To test for anchorage, independent growth cells were grown in 0.6% agar according to a modification of the method previously described.[45] Briefly, a stock of 1.2% Agar Noble (Gibco) was autoclaved and then the solution was equilibrated at 37°C for 60 min. The agar was diluted in RPMI medium (1:1), to form a basal layer, and 1 ml of the mixture was added to each well of a six-well plate. The basal layer solidified at 4°C in 15 min, which was subsequently rebalanced at room temperature for 30 min. PC-3 and LNCaP cell lines (1×10^5) suspended in complete RPMI medium with 20% FBS containing 0.3% agar noble were laid on the semi-solid bottom layer. For 15 min, the plates were kept at room temperature and then incubated for 24 h (37°C, 95% O_2, 5% CO_2). The next day, 1 ml of medium with compound **10** at its cytotoxic IC_{50} concentrations was added to each well (Table 2). The cells were dyed with crystal violet (0.01%) for 18 h at 37°C, after 2 weeks of incubation. A light microscope was used to take the pictures. The experiments were performed in triplicate.[11,22,46]

4.2.6 | Toxicological effect on brine shrimps

The toxicity bioassay was carried out using brine shrimp (*Artemia salina*) according to a modification of a method previously described.[39] In brief, artificial seawater was prepared by dissolving sea salt in distilled water (0.65 M). Then, seawater was added and a teaspoon of brine shrimp eggs was added and deposited in a small tank covered in one half. The other side of the tank was not covered to allow light, which attracted the hatched shrimps. The tank with the brine shrimp eggs was kept at room temperature for 24 h to promote the hatching of the eggs. Compound **10** was dissolved in DMSO, diluted with artificial seawater, so that the final concentration of DMSO did not exceed 0.05%. Different concentrations (50 µl, 15 µM–1.0 mM) of the compound were prepared; the test was performed in triplicate, in 96-well plates.[47] The brine shrimp larvae (nauplii, 10–20, 150 µl) were added to each well, covered with parafilm, leaving at room temperature for 24 h, after which the number of dead and surviving brine shrimps was determined using a light microscope. The experiment was replicated three times. Results are expressed as 50% lethal concentration (LC_{50}) values for the brine shrimp assay using probit analysis. The mortalities were corrected for the natural mortality observed in the negative controls using Abbott's formula, $p = \text{pi} - C/1 - C$, where pi denotes the observed control mortality rate and C denotes the natural mortality in treated shrimps.[11,46,47] The TAR is defined by the value resulting from the LC_{50} divided by the IC_{50} cytotoxic value of compound **10** for PC-3, LNCaP, or MatLyLu cells.

4.3 | Statistical analysis

One-way analysis of variance and *t* tests for specific group comparisons were used for data analysis. Significance was only considered when $p < .05$ for all analyses. Data were expressed as mean (*SD*). The software used was GraphPad Prism 4.02.[48]

ACKNOWLEDGMENTS

The authors thank the Instituto de Investigaciones Farmacéuticas (IIF) and Consejo de Desarrollo Científico y Humanístico de la Universidad Central de Venezuela (CDCH-UCV).

CONFLICTS OF INTERESTS

The authors declare that there are no conflicts of interests.

ORCID

Katiuska E. Charris http://orcid.org/0000-0002-8040-8318
Juan R. Rodrigues http://orcid.org/0000-0003-2399-6165
Hegira Ramírez http://orcid.org/0000-0003-1916-6118
Esteban Fernandez-Moreira http://orcid.org/0000-0003-1892-5370
Jorge E. Ángel http://orcid.org/0000-0002-2423-3285
Jaime E. Charris http://orcid.org/0000-0003-4404-2619

REFERENCES

[1] WHO report on cancer: Setting priorities, investing wisely and providing care for all. Geneva: World Health Organization; **2020**. Licence: CC BY-NC-SA 3.0 IGO.
[2] R. Siegel, K. Miller, H. Fuchs, A. Jemal, *CA–Cancer J. Clin.* **2021**, *71*, 7.
[3] J. Ferlay, M. Colombet, I. Soerjomataram, C. Mathers, D. Parkin, M. Piñeros, A. Znaor, F. Bray, *Int. J. Cancer* **2019**, *144*, 1941.
[4] Ä. Rana, J. Alex, M. Chauhan, G. Joshi, R. Kumar, *Med. Chem. Res.* **2015**, *24*, 903.
[5] W. Zheng, Y. Zhao, Q. Luo, Y. Zhang, K. Wu, F. Wang, *Curr. Top. Med. Chem.* **2017**, *17*, 3084.
[6] M. Islam, C. Wang, Z. N. Paudyal, Y. Zhu, H. Sun, *Eur. J. Med. Chem.* **2019**, *162*, 109.
[7] C. Huggins, C. Hodges, *Cancer Res.* **1941**, *1*, 293.
[8] I. Asangani, V. Dommeti, X. Wang, R. Malik, M. Cieslik, R. Yang, J. Escara-Wilke, K. Wilder-Romans, S. Dhanireddy, C. Engelke, M. Iyer, X. Jing, Y. Wu, X. Cao, Z. Qin, S. Wang, F. Feng, A. Chinnaiyan, *Nature* **2014**, *510*, 278.
[9] B. Liu, L. Su, J. Geng, J. Liu, G. Zhao, *ChemMedChem* **2010**, *5*, 1651.
[10] A. Patravale, A. Gore, D. Patil, G. Kolekar, M. Deshmukh, P. Anbhule, *Ind. Eng. Chem. Res.* **2014**, *53*, 16568.
[11] G. Mata, J. Rodrigues, N. Gamboa, K. Charris, G. Lobo, M. Monasterios, M. Avendaño, M. Lein, K. Jung, C. Abramjuk, B. Nitzsche, M. Hopfner, J. Charris, *Lett. Drug Des. Discov.* **2017**, *14*, 398.
[12] E. Nasr, A. Mostafa, M. El-Sayed, M. Massoud, *Arch. Pharm. Chem. Life Sci.* **2019**, *352*, e1800355.
[13] X. Song, J. Fan, L. Liu, X. Liu, F. Gao, *Arch. Pharm. Chem. Life Sci.* **2020**, *353*, e2000025.
[14] J. Nemeth, R. Yousif, M. Herzog, M. M. Che, J. Upadhyay, B. Shekarriz, S. Bhagat, C. Mullins, R. Fridman, M. Cher, *J. Natl. Cancer Inst.* **2002**, *94*, 17.
[15] M. Burg-Roderfeld, M. Roderfeld, S. Wagner, C. Henkel, J. Grotzinger, E. Roeb, *Int. J. Oncol.* **2007**, *30*, 985.
[16] L. Yang, W. Zeng, D. Li, R. Zhou, *Oncol. Rep.* **2009**, *22*, 121.
[17] A. Laghezza, G. Luisi, A. Caradonna, A. Di Pizio, L. Piemontese, F. Loiodice, M. Agamenonne, P. Tortorella, *Bioorg. Med. Chem.* **2020**, *28*, 115257.
[18] E. Lencia, A. Continib, A. Trabocchi, *Bioorg. Med. Chem. Lett.* **2020**, *30*, 127467.
[19] T. Turpeenniemi-Hujanen, *Biochimie* **2005**, *87*, 287.
[20] B. Bauvois, *Biochim. Biophys. Acta* **2012**, *1825*, 29.
[21] W. Stetler-Stevenson, A. Yu, *Semin. Cancer Biol.* **2001**, *11*, 143.
[22] J. Rodrigues, J. Charris, R. Ferrer, N. Gamboa, J. Ángel, B. Nitzsche, M. Hoepfner, M. Lein, K. Jung, C. Abramjuk, *Invest. New Drugs* **2012**, *30*, 1426.
[23] G. Kumar, B. Nair, J. Perry, D. Martin, *Med. Chem. Commun.* **2019**, *10*, 2024.
[24] J. Son, S. Lee, *Bioorg. Med. Chem. Lett.* **2020**, *30*, 127223.
[25] S. Kambe, K. Saito, A. Sakurai, H. Midorikawa, *Synthesis* **1980**, *1980*, 366.
[26] F. Shi, S. Tu, F. Fang, T. Li, *ARKIVOC* **2005**, *2005*, 137.
[27] M. Jachak, D. Kendre, A. Avhale, R. Toche, R. Sabnis, *J. Heterocycl. Chem.* **2007**, *44*, 1525.
[28] L. Rong, H. Han, H. Jiang, S. Tu, *J. Heterocycl. Chem.* **2009**, *46*, 465.
[29] X. Wang, X. Zeng, Y. Lie, D. Shi, S. Tu, X. Wei, Z. Zong, *Synth. Commun.* **2005**, *35*, 1915.
[30] Z. Ren, W. Cao, W. Tong, *Synth. Commun.* **2002**, *32*, 3475.
[31] B. Karmakar, B. Chowdhury, J. Banerji, *Catal. Commun.* **2010**, *11*, 601.
[32] B. Lee, K. Moon, J. Lim, Y. Park, D. Kim, S. Son, H. Jeong, D. Kim, E. Lee, K. Chung, H. An, P. Chun, A. Seo, J. Yang, B. Lee, J. Ma, W. Cho, H. Moon, H. Chung, *Oncotarget* **2017**, *8*, 91481.
[33] K. Makowska, M. Estañ, I. Gañán-Gómez, M. Boyano-Adánez, A. García-Pérez, P. Sancho, *Mol. Biol.* **2014**, *48*, 359.
[34] Y. Pan, S. Zhao, F. Chen, *Clin. Exp. Pharmacol. Physiol.* **2021**, *48*, 445.
[35] L. Rodríguez, X. Wu, J. Guan, *Methods Mol. Biol.* **2005**, *294*, 23.
[36] G. Morgia, M. Falsaperla, G. Malaponte, M. Madonia, M. Indelicato, S. Travali, M. Mazzarino, *Urol. Res.* **2005**, *33*, 44.
[37] V. Freedman, S. Shin, *Cell* **1974**, *3*, 355.
[38] U. Kelavkar, J. Nixon, C. Cohen, D. Dillehay, T. Eling, K. Badr, *Carcinogenesis* **2001**, *22*, 1765.
[39] J. McLaughlin, C. Chang, D. Smith, *Studies in Natural Product Chemistry* (Ed: A. Rahman), Vol. 9, Elsevier, Amsterdam **1991**, pp. 383.
[40] S. Park, J. Lee, S. Lee, *Cell Biochem. Biophys.* **2018**, *76*, 255.
[41] F. Denizot, R. Lang, *J. Immunol. Methods* **1986**, *89*, 271.
[42] Y. Ruiz, J. Rodrigues, F. Arvelo, A. Usubillaga, M. Monsalve, N. Diez, I. Galindo-Castro, *Phytochemistry* **2008**, *69*, 432.
[43] J. Atienza, J. Zhu, X. Wang, X. Xu, Y. Abassi, *J. Biomol. Screening* **2005**, *10*, 795.
[44] X. Qu, Y. Yuan, W. Xu, M. Chen, S. Cui, H. Meng, Y. Li, M. Makuuchi, M. Nakata, W. Tang, *Anticancer Res.* **2006**, *26*, 3573.
[45] A. Powell, S. Akare, W. Qi, P. Herzer, S. Jean-Louis, R. Feldman, J. Martinez, *BMC Cancer* **2006**, *6*, 219.
[46] J. Rodrigues, J. Charris, J. Camacho, A. Barazarte, N. Gamboa, F. Antunes, *Anticancer Res.* **2012**, *32*, 2721.
[47] P. Solis, C. Wright, M. Anderson, M. Gupta, J. Phillipson, *Planta Med.* **1993**, *59*, 250.
[48] GraphPad Prism Software Inc. 4.02 for Windows. May 17th (**1992–2004**).

SUPPORTING INFORMATION

Additional Supporting Information may be found online in the supporting information tab for this article.

How to cite this article: K. E. Charris, J. R. Rodrigues, H. Ramírez, E. Fernandez-Moreira, J. E. Ángel, J. E. Charris. Synthesis of 5*H*-indeno[1,2-*b*]pyridine derivatives: Antiproliferative and antimetastatic activities against two human prostate cancer cell lines. *Arch. Pharm.* 2021;e2100092. https://doi.org/10.1002/ardp.202100092